Global Model of a Negative Hydrogen Ion Source with Caesiated Plasma Grid

Sergey N. Averkin, Madhusudhan Kundrapu, Seth A. Veitzer
Tech-X Corporation, Boulder, CO U.S.A
Jonathan Smith
Tech-X UK Ltd, Daresbury, Cheshire UK

TECH-X CORPORATION

TuePE3

Introduction

Numerical models of chemically reacting plasmas such as in negative hydrogen ion sources (NHIS) span from detailed kinetic models (e.g. Particle-In-Cell method coupled with Direct Simulation Monte Carlo) to fluid models (e.g. Magnetohydrodynamics coupled with electromagnetic solvers), and then further to simple 0D or volume-averaged global models. Kinetic solvers provide detailed information about distribution functions of plasma components but have significant computational costs. Fluid models coupled with electromagnetic solvers can still provide detailed information about space and time distribution of plasma parameters with a reduced computational costs compared to kinetic solvers. However, the parametric investigation that can be used to model device optimization is still challenging task. For such reasons global models are widely used to perform quick simulations to extract most important chemical reactions and species information that can be further used in detailed fluid simulations. Our ultimate research goal is to provide the means to accurately model NHIS designs over a wide range of parameters using commercial code USim.

USim is a flexible fluid simulation code for solving a variety of continuum equations including fluids, plasmas, and electromagnetics. USim utilizes finite volume and discontinuous Galerkin techniques for solving equations on unstructured meshes with embedded geometries. We have used the USim simulation code to model a number of different ion sources, including the Spallation Neutron Source (SNS) internal antenna source, the next generation SNS external antenna negative hydrogen ion source, and the GEC benchmark Argon test source. We present preliminary results here describing the determination of the relevant reactive plasma species and chemistry channels for the production of H^- in a representative negative hydrogen source. These reactions will eventually be used in the USim fluid simulation model.

Global Model of a Negative Hydrogen Ion Source

We use a global model based on the Global Enhanced Vibrational Kinetic Model (GEVKM) to simulate a representative negative hydrogen ion source. The main assumptions of the global model:

(a) the domain is cylindrical with radius R and length L;
(b) all species have Maxwellian distribution functions;
(c) heavy species have the same temperature T_h, that is different from the electron temperature T_e;
(d) the electron and heavy species temperatures are uniform in the chamber;
(e) the number densities of all species are symmetric and can be decomposed as $n_p(r,z)=n_{p0}\Theta_{R,p}(r)\ \Theta_{L,p}(z)$, where n_{p0} is the number density of the component p at the center of the discharge, and $\Theta_{R,p}(r)$ and $\Theta_{L,p}(z)$ are non-dimensional profiles;
(f) plasma is quasineutral.

Governing Equations

The volume-averaged continuity equations for all species except electrons, quasineutrality condition, electron energy, and total energy equations are solved using the Newton-Raphson method for steady state number densities and temperatures

$$Q_p^{\rm in}-Q_p^{\rm out}-\frac{A}{V}\Gamma_p^{\rm wall}+\sum_r k_r\Omega_r\prod_p(\nu'_{r,p}-\nu_{r,p})\bar{n}_p^{\nu_p}=0,$$

$$\sum_{p,q_p\neq 0}q_p\bar{n}_p=0,$$

$$\frac{5}{2}k_B(T_e^{\rm out}Q_e^{\rm out}-T_e^{\rm in}Q_e^{\rm in})+k_B(T_h-T_e)\sum_h 2\frac{m_e}{m_h}\nu_{eh}^{\rm el}\bar{n}_e$$

$$+\frac{A}{V}\sum_{p,q_p>0}\Gamma_p^{\rm wall}(2k_BT_e+eV_p+eV_{\rm sh})$$

$$-\sum_r E_{r,\rm th}k_r\Omega_r\prod_p(\nu'_{r,p}-\nu_{r,p})\bar{n}_p^{\nu_{r,p}}=\frac{P_{\rm abs}}{V},$$

$$\sum_p\left[(U_{p,\rm kin}^{\rm in}+H_p^{\rm in})Q_p^{\rm in}-\left(U_{p,\rm kin}^{\rm out}+H_p^{\rm out}\right)Q_p^{\rm out}\right]+\frac{P_{\rm abs}}{V}=\frac{A}{V}q_{\rm wall}.$$

Chemical Reactions

The model includes electrons, neutral hydrogen molecules in all vibrational states $H_2(v)$, v=0-14, hydrogen atoms in the first 3 electronic states $H(n)$, and ground state ions H^+, H_2^+, H_3^+ and H^- and more than 1,000 of vibrationally resolved surface and volume chemical.

1. $e+H_2\rightarrow e+H_2^++e$
2. $e+H_2\rightarrow e+H+H$
3. $e+H_2\rightarrow H+H^-$
4. $e+H_2\rightarrow e+H^++H+e$
5. $e+H\rightarrow e+H^++e$
6. $e+H^-\rightarrow e+H+e$
7. $e+H_2^+\rightarrow H+H$
8. $e+H_2^+\rightarrow e+H+H^+$
9. $e+H_3^+\rightarrow 3H$
10. $e+H_3^+\rightarrow H+H_2$
11. $e+H_3^+\rightarrow H_2^++H^-$
12. $e+H_3^+\rightarrow e+H+H+H^+$
13. $H_2+H_2\rightarrow H_2+2H$
14. $H+H_2\rightarrow H+2H$
15. $H_2+H^+\rightarrow H_3^++h\nu$
16. $H_2+H^+\rightarrow H_2^++H$
17. $H_2+H_2^+\rightarrow H+H_3^+$
18. $H+H_2^+\rightarrow H_2+H^+$
19. $H^-+H\rightarrow e+H_2$
20. $H^-+H\rightarrow e+H+H$
21. $H^-+H_2\rightarrow H+H_2+e$
22. $H^-+H^+\rightarrow H+H$
23. $H^-+H^+\rightarrow H_2^++e$
24. $H^-+H_2^+\rightarrow H_2+H$
25. $H^-+H_2^+\rightarrow 3H$
26. $H^-+H_2^+\rightarrow H_3^++e$
27. $H^-+H_3^+\rightarrow H_2+2H$
28. $H^-+H_3^+\rightarrow H_2+H_2$
29. $H^-+H_3^+\rightarrow 4H$
30. $H_2+H+H\rightarrow H_2+H_2(v=14)$
31. $H+H+H\rightarrow H+H_2(v=14)$
32. $H^++2H_2\rightarrow H_3^++H_2$
33. $e+H_2(X^1\Sigma_g^+,v)\rightarrow H_2^-\rightarrow e+H_2(X^1\Sigma_g^+,v')$
34. $e+H_2(X^1\Sigma_g^+,v)\rightarrow e+H_2(B^1\Sigma_u^+,C^1\Pi_u)\rightarrow e+H_2(X^1\Sigma_g^+,v')+h\nu$
35. $e+H_2(v)\rightarrow H_2^-\rightarrow e+H_2(X^1\Sigma_g^+)\rightarrow e+H+H$
36. $e+H_2(v)\rightarrow H_2^-\rightarrow e+H_2(b^3\Sigma_g^+)\rightarrow e+H+H$
37. $e+H_2(v)\rightarrow e+H_2(b^3\Sigma_u^+,a^3\Sigma_g^+,c^3\Pi_u,\text{singlets})\rightarrow e+H+H$
38. $e+H_2(v)\rightarrow H_2^-\rightarrow H+H^-$
39. $H_2(v)+H_2(w)\rightarrow H_2(v+1)+H_2(w-1)$
40. $H_2(v)+H_2(w)\rightarrow H_2(v\pm 1)+H_2(w)$
41. $H_2+H_2(v)\rightarrow H_2+2H$
44. $H^++H_2(v)\rightarrow H+H_2^+$
45. $H^-+H_2(v)\rightarrow H_2(v-2)+H+e,\ (2\leq v\leq 6)$
46. $e+H\rightarrow e+H(n=2,3)$
47. $e+H_2\rightarrow e+H+H(n=2,3)$
48. $e+H(n=2,3)\rightarrow e+H^++e$
49. $H(n=3)\rightarrow H(n=2)+h\nu$
50. $H(n=2,3)+H_2\rightarrow H_3^++e$
51. $H(n=2,3)+H_2\rightarrow 3H$
52. $H+H+\text{wall}\rightarrow H_2$
53. $H_2(v)+\text{wall}\rightarrow H_2(v)$
54. $H^++\text{wall}\rightarrow H$
55. $H_2^++\text{wall}\rightarrow H_2$
56. $H_3^++\text{wall}\rightarrow H+H_2$
57. $H(n)+\text{wall}\rightarrow H$

Global model parameters

We consider a cylindrical ICP source with R=20 cm, L=74.5 cm. The parameters of this representative ion source were chosen to resemble negative hydrogen ion source developed at IPP Garching. We assumed that the extraction grid consists of 625 holes with radius r=4.4 mm corresponding to the total extraction area of 0.038 m^2.The volumetric inlet flow rate of pure H_2 is considered to be 1.5 slm while absorbed power was taken in the range from 10 kW to 100 kW. The estimated mean free path of plasma components $\lambda_i \ll 2r$. Therefore, we used mean free path theory to calculate outlet flow rates. The ion source wall temperature was taken at fixed temperature 300 K. These parameters were chosen to result in the pressure 0.3 Pa in the negative hydrogen ion source without plasma turned on.

Simulation results of cesium free operation

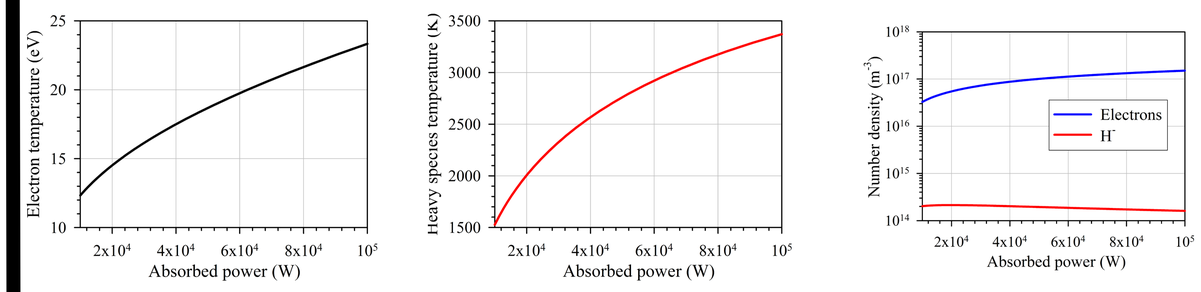

Left and center figures above show electron and heavy species temperatures as a function of absorbed power at constant inlet flow rate. The increase in absorbed power leads to monotonic increase in both electron and heavy species temperatures. At 10 kW the electron temperature is close to 12 eV while heavy species temperature is 1500 K. At 100 kW the electron temperature reaches 23 eV and heavy species temperature is close to 3400 K. These results are consistent with 2D fluid simulations of the ITER negative hydrogen ion source. Right figure above depicts number densities of electrons and negative hydrogen ions in a range of absorbed power from 10 kW to 100 kW and inlet flow rate 1.5 slm. At these operating conditions the number density of H^- is almost two orders of magnitude smaller than those of electrons.

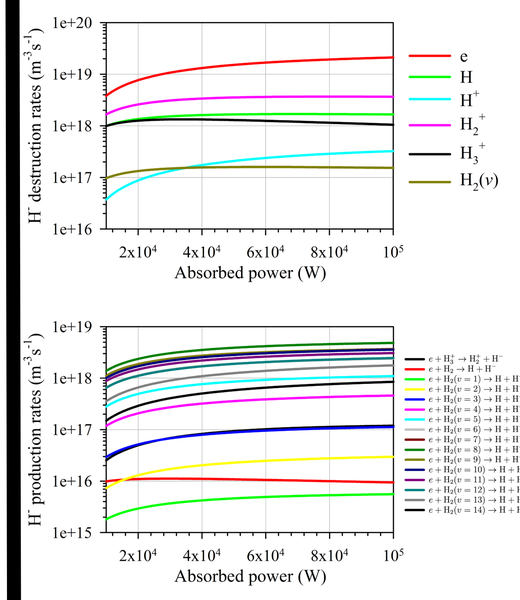

To better understand the production and destruction processes that lead to observed number densities of negative hydrogen ions production and destruction rates are shown above. The main production mechanism in the cesium free negative hydrogen ion source is due to dissociative electron attachment to high lying vibrationally excited hydrogen molecules ($8\leqslant v\leqslant 11$). The dominant destruction process is due to collisions of H^- with electrons. At absorbed power 10 kW the electrons contribute 50 % of the total destruction rate while at 100 kW they contribute around 90 % to the total destruction rate.

Top figure on the right presents atomic and molecular hydrogen number densities as a function of absorbed power. In this source configuration the degree of dissociation increases from 1% at absorbed power of 10 kW to 25% at absorbed power of 100 kW that is consistent with 2D fluid simulations in ITER source.

The number densities of positive ions as a function of absorbed power are presented in the bottom figure on the right. At all considered absorbed powers the dominant positive ion is H_2^+. At absorbed powers below 36 kW the number density of H_3^+ is higher than of H^+. As absorbed power increases the number densities of all positive ions monotonically increase.

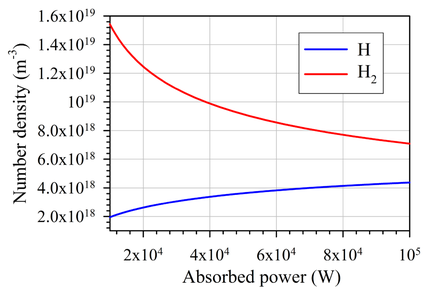

Simulation results of operation with cesium addition

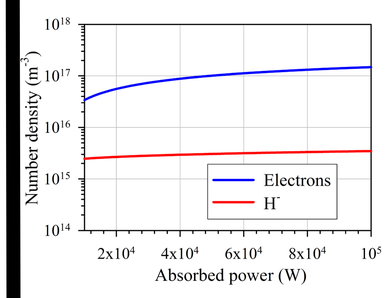

Assuming 0.011 m^2 as the total area of the surface covered by cesium and 20 % conversion probability of H and H^+, the number density of H^- is almost one order of magnitude higher as can be seen from the figure on the left. Other parameters such as electron and heavy species temperatures, number densities of other components didn't change. It should be noted that in the real negative hydrogen source the increased number density of H^- will be mainly localized near the grid.

Tech-X Corporation, Boulder, CO

This work was performed under the auspices of the Department of Energy, Office of Basic Energy Sciences Award #DE-SC0009585

ICIS'17
CERN – CIGG –Geneva, Switzerland, 15-20 October, 2017.